

MU-MIMO Uplink Timely Throughput Maximization for Extended Reality Applications

Ravi Sharan B A G, K. Pavan Srinath, Alvaro Valcarce Rial, and Baltasar-Beferull Lozano

Abstract

In this work, we study the cross-layer timely throughput maximization for extended reality (XR) applications through uplink multi-user MIMO (MU-MIMO) scheduling. Timely scheduling opportunities are characterized by the peak age of information (PAoI)-metric and are incorporated into a network-side optimization problem as constraints modeling user satisfaction. The problem being NP-hard, we resort to a signaling-free, weighted proportional fair-based iterative heuristic algorithm, where the weights are derived with respect to the PAoI metric. Extensive numerical simulation results demonstrate that the proposed algorithm consistently outperforms existing baselines in terms of extended reality (XR) capacity without sacrificing the overall system throughput.

Index Terms

6G Communications, Proportional fair scheduling, Peak AoI, XR, MU-MIMO

Preprint Notice: This work has been submitted to the IEEE for possible publication. Copyright may be transferred without notice, after which this version may no longer be accessible.

I. INTRODUCTION

XR services encompassing mixed (augmented) reality (MR) and virtual reality (VR) technologies are shaping the future immersive multimedia applications. A seamless XR experience over

Ravi Sharan is with Nokia Bell Labs, Germany. K. P. Srinath and Alvaro V. Rial are with Nokia Bell Labs, France. Email: {ravi.bhagavathula, pavan.koteshwar_srinath, alvaro.valcarce_rial}@nokia-bell-labs.com. Baltasar B. Lozano is with SimulaMet and University of Agder, Norway. Email : baltasar@simula.no. Part of this work was carried out when Ravi Sharan was enrolled as a PhD student at the University of Agder, Norway.

wireless cellular networks involve delivering high and reliable data rates ($\approx 30 - 150$ Mb/s) with low latencies ($\approx 5 - 30$ ms). These requirements are further amplified in co-located multi-user MR scenarios, where users simultaneously interact with one another and their virtual environments. Regardless, MR applications are equally intensive in the uplink (UL) as they are in the downlink (DL). This is because a user equipment (UE) continuously transmits raw video for 3D-rendition at the radio access network (RAN) [1]. Thus, UL optimization plays a crucial role in realizing the full potential of these XR services.

For delivering a guaranteed quality of service (QoS) in the UL, UE scheduling with delay-specific information is currently being considered in the third generation partnership project (3GPP) studies [2]. Quality of experience (QoE) is handled separately by extracting application awareness at the video frame-level and embedding it into the medium access control (MAC) layer as packet-level metadata [3]. On the other hand, with latest advances in the physical (PHY) layer, multi-user multiple input multiple output (MU-MIMO) is being seriously investigated for sixth generation (6G) networks [4]. UE scheduling in MU-MIMO becomes extremely challenging due to intra-cell interference, which impacts precoding at the PHY layer and consequently the Qo(S)E. Thus, a careful consideration of both PHY-MAC aspects is imperative for MU-MIMO UL scheduling in XR applications.

Scheduling schemes based on the well known proportional fair (PF) metric are widely adopted in the commercial fifth generation (5G) cellular networks [5]. The PF metric aims to maximize the system throughput based on the channel conditions while maintaining long-term fairness among the UEs. Going forward, Qo(S)E-related extensions to the PF metric are necessary to successfully employ it in XR scenarios. However, acquiring the aforementioned application awareness information involves additional signaling overhead in the UL and cannot be fully generalized across applications. *In this work, we follow a signaling-free approach and employ age of information (AoI) alongside PF metric for MU-MIMO UL UE scheduling in a XR scenario.* The AoI is defined as the time elapsed since a UE's last generated successful packet, where it jointly captures the inter-delivery times and the packet-delays [6]. Furthermore, we use the peak AoI (PAoI) metric to model the Qo(S)E of the UEs, since it can be easily coupled with the packet delay budget (PDB) [7]. To the best of our knowledge, we are not aware of existing works on AoI-aware UL scheduling with XR traffic considering full-blown MU-MIMO PHY aspects.

Related Literature: Current literature on XR UE scheduling heavily focuses on DL single-

user MIMO (SU-MIMO) scenarios. For instance, the work in [8] proposed a QoS-aware scheduling heuristic algorithm for XR and 5G eMBB traffic. Here, the scheduling metric is modeled with respect to the recently introduced protocol data unit (PDU)-set concept. The authors in [9] propose two scheduling heuristic algorithms to maximize the number of satisfied XR UEs by combining multiple video frames into one entity. The work in [10] proposed a signaling-aided scheme to meet the target Qo(S)E and XR key performance indicators (KPIs), where the gNodeB (gNB) collects periodic measurements from the UEs. Above schemes exploit packet-level metadata to model the DL scheduling metrics, which can be hard to incorporate in UL UE scheduling without introducing additional signaling overhead. Firstly, the signaling overhead can have a detrimental effect on the achievable Qo(S)E under stringent latency requirements of the XR applications. Even if the signaling is well-handled, intra-cell interference poses an additional challenge for UE scheduling in MU-MIMO.

On the other hand, AoI-aware UL scheduling for short-packet communications with single-antenna UEs are explored in [11] and [12]. The work in [11] proposes a deep reinforcement learning (DRL) solution for throughput maximization subject to network-wide sum-AoI constraint in a SU-MIMO setting. Finally, an interference-approximated whittle-index policy is proposed to minimize the network-wide sum-AoI subject to instantaneous deadline in [12]. However, these works do not shed light on the AoI behavior under XR traffic. Within this context, we now present the system model, which is followed by problem formulation, proposed solution and numerical results.

II. SYSTEM MODEL

We consider a MU-MIMO scenario with a single gNB serving N XR UEs in the UL. Let $\mathcal{N} := \{1, 2, \dots, \bar{N}\}$, $|\mathcal{N}| = \bar{N}$ denote the set of all UEs served by the gNB. A subset of UEs from \mathcal{N} are multiplexed together during a single transmission opportunity in the same time-frequency 2D resource grid. In the time-domain (TD), the transmission opportunity is represented by transmission time interval (TTI) $t \in \mathcal{T} \subseteq \mathbb{N}^+$. A TTI comprises N_{sym} orthogonal frequency division multiplexing (OFDM) symbols. In the frequency axis, there are F resource blocks (RBs) with each RB $f \in \mathcal{F} := \{1, 2, \dots, F\}$ spanning N_{sc} sub-carriers. Thus, for every TTI t , there are a total of $I_f = N_{sc} \cdot N_{sym}$ resource elements (REs) per each RB f . Here, a RE is the smallest unit of the 2D resource grid. Furthermore, we assume that the gNB operates with N_G transceiver chains (TRX) and a UE $n, \forall n \in \mathcal{N}$ is equipped with N_U TRX w.l.o.g. At any TTI t , a UE

n operates with $\lambda_n(t) \leq N_U$ spatial streams of data. Consequently, the total number of spatial streams from the set of co-scheduled UEs, $\mathcal{N}'(t) \subseteq \mathcal{N}$ result in $\Lambda(t) = \sum_{n \in \mathcal{N}'(t)} \lambda_n(t)$. Moreover, there is an upper limit of $\Lambda(t) \leq \bar{\Lambda} \leq N_G$ on the total number of spatial layers from $\mathcal{N}'(t)$ at any TTI t .

As for the wireless channel, we assume a flat and block fading channel, i.e., it remains constant for a single TTI t and varies across different TTIs in a correlated manner. Similarly, the channel is assumed to remain constant over a single RB f and vary across different RBs. The received complex signal vector $\mathbf{y}(i_f; t) \in \mathbb{C}^{N_G \times 1}$ at the gNB, at TTI t and on the RE $i_f \in \mathcal{I}_f := \{1, 2, \dots, I_f\}$ is given by:

$$\mathbf{y}(i_f; t) := \sum_{n \in \mathcal{N}'(t)} \mathbf{H}_n(f; t) \mathbf{x}_n(i_f; t) + \boldsymbol{\eta}(i_f; t). \quad (1)$$

In the above expression, $\mathbf{H}_n(f; t) \in \mathbb{C}^{N_G \times L_n(t)}$ is the effective UL channel between the UE u_n and the gNB. The effective channel is assumed to be estimated using known pilot symbols and subsumes the precoding operation. The term $\mathbf{x}_n(i_f; t) \in \mathbb{C}^{L_n(t) \times 1}$ is the data vector of UE u_n that is transmitted on the RE $(i_f; t)$. Finally, $\boldsymbol{\eta}(i_f; t) \in \mathbb{C}^{N_G \times 1}$ collectively denotes the inter-cell interference (if any) plus thermal noise with mean $\mathbf{0}$ and covariance matrix $\mathbf{R}_{cov} \in \mathbb{C}^{N_G \times N_G}$. Notice that the index for the effective channel matrix is with respect to f , compared to the remaining terms, which is a consequence of the assumptions on the channel above. The post equalization effective signal-to-interference-plus-noise ratio (SINR) estimate of a UE n on RE i_f , denoted by $\rho_n(i_f; t)$, is obtained as a function of $\mathbf{H}_n(f; t)$, $\mathbf{H}_{n'}(f; t)$, $\forall n' \in \mathcal{N}'(t) \setminus \{n\}$ and \mathbf{R}_{cov} (expression omitted here due to space constraints, see [13, Eq. (5)]). The *achievable throughput* of a UE n , denoted by $Q_n(t) \in \mathbb{R}_{\geq 0}$, can then be approximated [13] as follows:

$$Q_n(t) \leq \lambda_n(t) \cdot \left(\sum_{f \in \mathcal{F}} \sum_{i_f \in \mathcal{I}_f} \log_2(1 + \hat{\rho}_n(i_f; t)) \right), \quad (2)$$

where, $\hat{\rho}_n(i_f; t)$ represents the transmit power scaled SINR.

Following sequence of operations ensue at the gNB. At the beginning of a TTI t , all the associated UEs send their buffer status report (BSR) $b_n(t) \in \mathcal{B} := [0, \bar{B}_n]$ to the gNB indicating the number of bits pending transmission. Here, \bar{B}_n denotes the maximum allowable size of a packet. The term packet is used in this work to refer to a data-burst in 3GPP XR specifications, which comprises multiple PDUs grouped together with respect to the underlying video frames with periodic arrivals. The gNB then selects a subset of UEs and for each $n \in \mathcal{N}'(t)$ indicates the scheduling decision using a binary variable $\beta_n(t) = 1$. The gNB also assigns the number of

spatial streams, $\lambda_n(t)$ and the modulation and coding scheme (MCS) value to be used by the co-scheduled UEs in $\mathcal{N}'(t)$. The co-scheduled UEs then perform RB selection, UL power control and transmit a fraction of the packet by means of transport blocks (TBs). The TB bit-size at a UE is proportional to its assigned MCS value. The gNB sends back an instantaneous feedback $s_n(t) \in \{0, 1\}$, upon successful/unsuccessful reception of the corresponding TBs. Note that we do not consider retransmissions in this work. The UEs update their BSR based on the $s_n(t)$ value and the process repeats over time.

Following packet generation and AoI modeling is considered in this work. A new packet of length B_n , s.t. $B_n \leq \bar{B}_n$ is generated at a UE n only when the current packet:

- (a) is either successfully received at the gNB or,
- (b) exceeds the PDB, \bar{D} leading to a packet failure.

Additionally, we assume that $B_n > Q_n(t), \forall n \in \mathcal{N}, \forall t \in \mathcal{T}$, implying that a UE takes several TTIs to successfully transmit its packet. A UE's AoI value, denoted by $\Delta_n(t) \in \mathbb{N}^+$, increases linearly with time and is reset to its default value (set to one in this work w.l.o.g) only when the UE is scheduled for transmission and the current packet is successfully transmitted. We also consider a finite-value clipping of the AoI beyond $\bar{\Delta}$, which is chosen to be greater than \bar{N} and \bar{D} . The gNB maintains a separate counter for each UE to track the AoI evolution, which can be formally expressed as:

$$\Delta_n(t+1) := \min(\Delta_n(t), \bar{\Delta}) \cdot (1 - \phi_n(t+1)) + 1. \quad (3)$$

Here, $\phi_n(t+1)$ is a joint Bernoulli random variable spanning the current and the next TTIs t and $t+1$ and models UE selection, TB-level instantaneous feedback and UE's packet replenishment (denoted by an indicator function with respect to the BSR below). Formally, it is given by:

$$\phi_n(t+1) := \begin{cases} 1, & \text{if } \beta_n(t) \wedge s_n(t) \wedge \mathbb{1}_{\{b_n(t+1) > b_n(t)\}} = 1 \\ 0, & \text{otherwise.} \end{cases} \quad (4)$$

The significance of the joint condition in (4) is that the gNB can deduce whether a UE's packet replenishment has occurred due to condition (a) or (b) from the above packet generation model. This also alleviates any need for explicit packet-level metadata other than the BSR to be exchanged between UEs and the gNB for UL UE scheduling in XR applications.

Besides AoI modeling, we consider the time-averaged PAoI as a metric to effectively evaluate the Qo(S)E and the XR KPI. Denoted by $\Delta_{n,PAoI}$, the time-averaged PAoI is the average of AoI values right before $\phi_n(t) = 1$. Formally, $\Delta_{n,PAoI}$ can be expressed as:

$$\Delta_{n,PAoI} := \frac{\sum_{\mathcal{T}} \Delta_n(t)}{\sum_{\mathcal{T}} \phi_n(t+1)} \quad (5)$$

Based on the above assumptions and modeling, we now present the optimization problem considered in this work.

III. TIMELY THROUGHPUT MAXIMIZATION

Maximizing the number of satisfied UEs in the network, termed XR capacity, constitutes an important XR KPI, where a UE is labeled satisfied if at least 99% of its packet is successfully received within the PDB [1]. For the system model outlined in section II, the above KPI can be partially addressed by maximizing the system throughput through fair UE scheduling. On top of this, UE satisfaction can be incorporated using timely scheduling opportunities through the PAoI metric defined in (5). The throughput achieved in this manner is concisely referred to as the *timely throughput* in this work and is formally expressed using the optimization problem below:

$$\mathbf{P1:} \underset{\boldsymbol{\beta}(t); \forall t}{\text{maximize}} \quad \limsup_{T \rightarrow \infty} \frac{1}{T} \sum_{\mathcal{T}} \sum_{\mathcal{N}} \beta_n(t) \cdot U_{\alpha}(Q_n(t)) \quad (6a)$$

$$\text{subject to } \left\{ \limsup_{T \rightarrow \infty} \Delta_{n,PAoI} \leq \bar{D} \right\}_{n=1}^{\bar{N}}, \quad (6b)$$

$$\sum_{n \in \mathcal{N}} \lambda_n(t) \cdot \beta_n(t) \leq \bar{\Lambda}, \quad (6c)$$

$$\boldsymbol{\beta}(t) \in \{0, 1\}^{\bar{N}}, \forall n \in \mathcal{N}.$$

The problem posed in (6) is an integer non-linear programming problem involving time-averaged expressions in (6a) and (6b), along with instantaneous constraints in (6c). The optimization variable $\boldsymbol{\beta}(t) \in \{0, 1\}^{\bar{N}}$ is a binary vector indicating the co-scheduled UEs at TTI t . The function $U_{\alpha}(\cdot)$ in (6a) denotes the well-known α -fair utility function [14] which is used to enforce fairness with respect to UE scheduling. The interrelation between UEs' PAoI, $\Delta_{n,PAoI}$, $\forall n \in \mathcal{N}$ and the PDB, \bar{D} is captured by the constraint set in (6b). Such a coupling between PAoI and PDB is possible since the time instances when a UE's AoI is reset to its default value signifies a packet replenishment. Furthermore, we consider multiple per-UE constraints as opposed to a single

network-wide utility function of UEs' PAoI to better reflect the XR KPI. Finally, the coupling constraint (6c) ensures that the total number of spatial layers served by gNB does not exceed $\bar{\Lambda}$.

It can be observed that maximizing (6a) in isolation reduces **P1** to the classical fairness-enabled MU-MIMO throughput maximization solely with respect to the PHY layer aspects. However, inclusion of (6b) transforms **P1** into a cross-layer optimization problem delivering *timely and meaningful* packet throughput to the UEs within the PDB. From a solution perspective, **P1** seemingly looks like it can be decoupled across UEs by relaxing the coupling constraint in (6c). However, it is still not straightforward to decouple (6) since intra-cell interference acts as an implicit coupling constraint reflecting through $Q_n(t), \forall n \in \mathcal{N}$ computation. On top of this, the integer nature of the optimization variable $\beta(t)$ renders the above problem NP-hard. To effectively address these challenges, we propose a practically applicable, per-TTI iterative heuristic algorithm to solve (6), where the per-iteration decisions are evaluated using the PAoI-weighted PF metric.

IV. PROPOSED SCHEDULING HEURISTIC

It is evident from section III that a UE scheduling scheme solving (6) should efficiently manage between UE fairness, system throughput and PAoI constraint satisfaction. The widely adopted PF-metric-based schemes aim to strike a good balance between the first two attributes under different channel and interference conditions. As for (6), utilizing the PF-metric corresponds to the case when $\alpha = 1$ in $U_\alpha(\cdot)$ and renders (6a) as maximizing a network-wide sum of per-UE logarithmic utility of throughput at every TTI, i.e., $\sum_{n \in \mathcal{N}} \log(Q_n(t))$. While fairness can be further improved by setting $\alpha > 1$, it can potentially impede timely scheduling opportunities to UEs and impact the achievable Qo(S)E and the XR KPI. This is because UEs with worse channel conditions end up receiving a very high proportion of scheduling opportunities on an average in the TD as $\alpha \rightarrow \infty$. Additionally, it can also result in intra-cell interference and eventually leads to packet replenishment at UEs due to condition (b) of the packet generation model from section II. Considering all these, we employ a weighted PF-metric-based scheduling heuristic algorithm to solve (6), where the weights are derived as a function of PAoI metric of each UE.

In order to maximize (6a) on a per-TTI basis by setting $\alpha = 1$ in $U_\alpha(\cdot)$, i.e., $\sum_{n \in \mathcal{N}} \log(Q_n(t))$, one has to maximize $\sum_{n \in \mathcal{N}} \frac{Q_n(t)}{Q_{n,Avg}(t)}$ [14]. Here, $Q_n(t)$ is the per-UE achievable throughput at TTI t from (2), which is conditioned on the subset of co-scheduled UEs, $\mathcal{N}'(t)$. Furthermore, $Q_{n,Avg}(t)$ is a linear estimate of the per-UE achieved throughput until TTI t , for which the update

rule is given by:

$$Q_{n,Avg}(t+1) = (1 - \tau)Q_{n,Avg}(t) + \tau \cdot \beta_n(t) \cdot Q_n(t). \quad (7)$$

Here, τ is a time constant, whose value is typically chosen to be in the order of 1000 TTIs (e.g. $\tau = \frac{1}{1000}$). We now extend this to (6) and accommodate the constraint set (6b) in the PF-metric through a per-UE multiplicative weight, $W_{n,PAoI}(t)$ scaling $Q_{n,Avg}(t)$ as defined below:

$$W_{n,PAoI}(t) := \begin{cases} (\Delta_{n,wa}(t))^{-\kappa}, & \text{if } \Delta_{n,wa}(t) \leq \bar{D} \\ 1 - (\Delta_{n,wa}(t))^{-\kappa}, & \text{otherwise.} \end{cases} \quad (8a)$$

$$W_{n,PAoI}(t) := \begin{cases} (\Delta_{n,wa}(t))^{-\kappa}, & \text{if } \Delta_{n,wa}(t) \leq \bar{D} \\ 1 - (\Delta_{n,wa}(t))^{-\kappa}, & \text{otherwise.} \end{cases} \quad (8b)$$

Here, $\Delta_{n,wa}$ is the weighted average computed with respect to instantaneous AoI $\Delta_n(t)$ and the running average of the PAoI metric $\Delta_{n,PAoI}$ as:

$$\Delta_{n,wa}(t) := \theta \cdot \Delta_n(t) + (1 - \theta) \cdot \sum_{t'=0}^t \Delta_{n,PAoI}(t'). \quad (9)$$

The quantities $\kappa \in \mathbb{R}^+$ and $\theta \in [0, 1]$ are interdependent tunable parameters. For instance, κ assumes smaller values if $\Delta_{n,wa}(t)$ is prioritized and takes on higher values if $\sum_{t'=0}^t \Delta_{n,PAoI}(t')$ is prioritized in (9). Finally, (8) and (9) capture the R.H.S and L.H.S of (6b), respectively.

Besides modeling the AoI-weighted PF-metric, we also incorporate (6c) in our proposed scheduling heuristic algorithm by leveraging the interconnection between $\bar{\Lambda}$ and $\mathbf{\Lambda}$. More specifically, we identify that (6c) essentially translates into an upper bound on the number of UEs that can be co-scheduled in a TTI $N(t) \leq \bar{N}$, which can be approximated as follows:

$$N(t) := \left\lceil \frac{\bar{\Lambda}}{\frac{1}{\bar{N}} \sum_{n \in \mathcal{N}} \lambda_n(t)} \right\rceil, \implies \mathbf{1}^T \boldsymbol{\beta}(t) \leq N(t), \quad (10)$$

The pseudocode for the proposed scheduling heuristic algorithm is presented in Algorithm 1, where the term $Q_{sum}(\mathcal{N}'(t)) := \sum_{n \in \mathcal{N}'(t)} \frac{Q_n(t)}{Q_{n,Avg}(t) \cdot W_{n,PAoI}(t)}$. The proposed scheduling heuristic algorithm serves the subset of UEs which maximize Q_{sum} at each TTI t i.e., it prioritizes the UEs with a high $Q_n(t)$ value and a low value of the product $Q_{n,Avg} \cdot W_{n,PAoI}$. Thus, $W_{n,PAoI}$ in (8) guides the PF-metric to prioritize a UE until $\Delta_{n,wa}(t) \leq \bar{D}$, beyond which it linearly approaches the classical PF-metric. Thus, the proposed scheduling heuristic algorithm strikes a good balance between PAoI constraint satisfaction, system throughput and UE fairness.

Algorithm 1 Per-TTI Timely Throughput Maximization

Initialize: $\tau, \kappa, \theta, \bar{\Lambda}, \bar{D}$.

Input: $\Delta_{n,wa}(t), \mathbf{H}_n(f; t), \mathbf{R}(i_f; t), \forall i_f \in \mathcal{I}_f, \forall f \in \mathcal{F}, \forall n \in \mathcal{N}$.

```

1: Set  $\mathcal{N}'(t) \leftarrow \emptyset$ ,  $\mathcal{K}(t) \leftarrow \emptyset$ , and  $Q_{sum}(\mathcal{N}'(t)) \leftarrow 0$ .
2: for each  $n \in \mathcal{N}$  do
3:    $\mathcal{K}(t) \leftarrow \mathcal{N}'(t)$ 
4:   if  $Q_{sum}(\mathcal{N}'(t) \cup \{n\}) > Q_{sum}(\mathcal{N}'(t))$  then
5:      $\mathcal{N}'(t) \leftarrow \mathcal{N}'(t) \cup \{n\}$ 
6:      $Q_{sum}(\mathcal{N}'(t)) \leftarrow Q_{sum}(\mathcal{N}'(t) \cup \{n\})$ 
7:   end if
8:   if  $|\mathcal{N}'(t)| > N(t)$  OR  $\sum_{n \in \mathcal{N}'(t)} \lambda_n(t) > \bar{\Lambda}$  then
9:     return  $\mathcal{K}(t)$ .                                ▷ Early stopping rule.
10:  else Continue
11:  end if
12: end for
13: return  $\mathcal{N}'(t)$ .                                ▷ Equivalent to obtaining  $\beta(t)$  in (6).

```

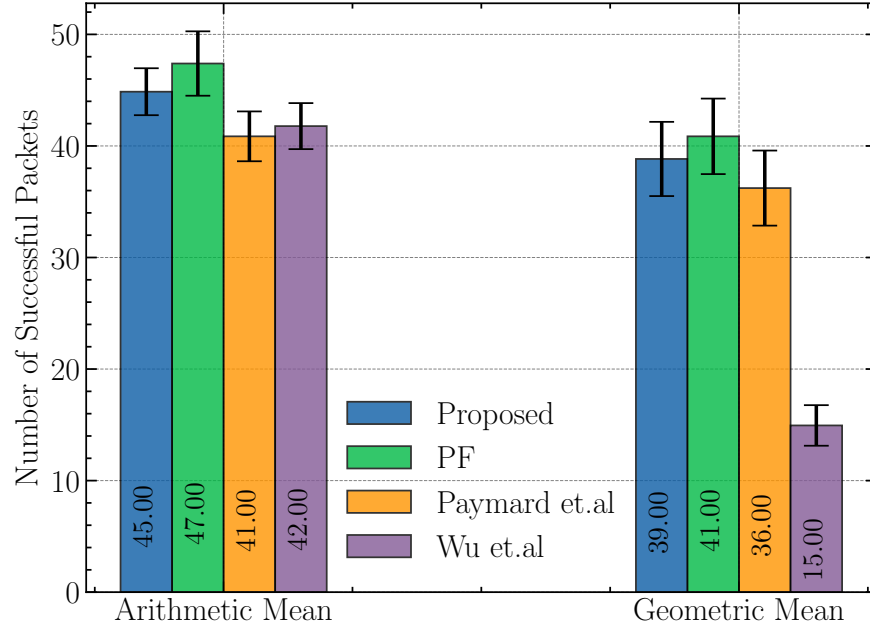


Fig. 1: Goodput comparison of top 95% UEs

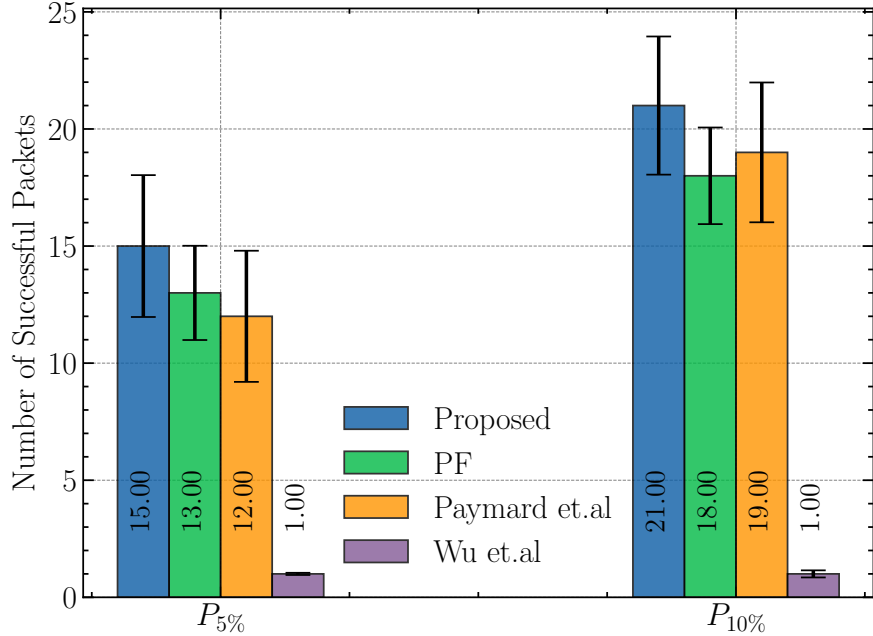


Fig. 2: Goodput comparison of bottom 5% and 10% UEs

V. NUMERICAL RESULTS

In this section, we evaluate the performance of Algorithm 1 using a multi-cell (gNB in this work), multi-link-level simulator written in NumPy (for channel estimation) and TensorFlow. We consider a single site with three gNBs, where each gNB is considered to serve $\bar{N} = 10$ UEs in MU-MIMO mode. Each gNB operates with 48 (3 \times 1 subarray) antenna elements and is configured with $N_G = 16$ -TRX (2H \times 4V \times 2P). Furthermore, we consider the maximum spatial layers the gNB can support at any TTI, $\bar{\Lambda} = 8$. The UEs are configured with $N_U = 4$ -TRX (2H \times 1V \times 2P). For PHY attributes, we consider the 3GPP 38.901-Urban Micro (UMi) NLoS channel model with 5G pilots for channel estimation. Other relevant PHY attributes such as UE transmit power, RB-settings, MCS table and channel coding parameters etc., can be found in [13, sec. 5, tbl. I]. Furthermore, we also follow the baseline UL power control, RB allocation and UE rank-selection from [13, sec. 5.A]. As for XR application attributes, we consider the packet-size, $B_n(t) = \bar{B} = 75000$ bits (9375 Bytes), $\forall n \in \mathcal{N}$ for simplicity in evaluation. The PDB value is selected as $\bar{D} = 30$ and consider an additional grace period of two TTIs beyond PDB. This is to provision UEs to send their final remaining TBs (if any) before packet replenishment. For the BSR reporting, we follow [15, tbl. 6.1.3.1-1]. Furthermore, the AoI clipping value is chosen

as $\bar{\Delta} = 100$. The tunable parameters from (8) and (9) are chosen as $\kappa = 2$ and $\theta = 0.5$. Finally, the simulations are run for 35 individual drops and a total of 10^6 TTIs. As for the baselines, we consider the DRL solution from [11] and adopt the classical PF-metric and the weighted PF metric in Algorithm 1.

We begin our evaluation in Figs. 1 and 2 by comparing the goodput in terms of average number of packet replenishments at the UEs with 90% confidence interval. Here, the averaging is performed with respect to both TTIs and the number of UEs and is rounded off to the nearest integer. For the top 95% UEs, the proposed scheduling heuristic outperforms the baseline schemes in [8] and [11] with respect to both arithmetic and geometric means as shown in Fig. 1. At the same time, the proposed scheduling heuristic achieves a comparable performance with respect to the PF baseline. On the other hand, for the bottom 5% and 10% or the cell-edge UEs, the proposed heuristic consistently outperforms all the baselines as depicted in Fig. 2. This shows that scaling the PF-metric by PAoI weights from (8) only slightly sacrifices the goodput of the top 95% UEs to accommodate the cell-edge UEs. Furthermore, this is accomplished efficiently, since cell-edge UEs transmit with low MCS values (potentially causing interference) and require more scheduling opportunities on an average for successful packet deliveries.

Next, we evaluate the XR capacity achieved by the proposed scheduling heuristic and the baselines in Fig. 3. More specifically, we compare the distributions of the time-averaged achieved PAoI of the UEs using a box plot figure. A box plot provides a compact distributional summary, where the data points are either partitioned into the quartiles or marked as outliers if they lie beyond the quartiles [16]. The term q in Fig. 3 represents the percentile of UEs that satisfy constraint (6b). Firstly, the proposed scheduling heuristic achieves the *highest* XR capacity of $q = 81\%$. This is a significant improvement over the classical PF scheduler, especially given that their goodput performance is comparable. Furthermore, a reasonable improvement in XR capacity with respect to the baseline in [8] is still significant, since the proposed scheduling heuristic follows a signaling-free approach unlike [8]. Secondly, the proposed scheduling heuristic achieves the *lowest* distributional mean of $\mu = 28$, which is well below the PDB. This is because the outliers with respect to the proposed scheduling heuristic are closer to the fourth quartile compared to the baselines, whose outliers have longer tail distributions. Furthermore, despite classical PF scheduler and the baseline in [8] achieving a mean close to the PDB, their XR capacity is still not maximized due to longer tail distributions. This asserts the need for per-UE constraints in (6b) as opposed to the network-wide sum PAoI minimization. Finally, it can

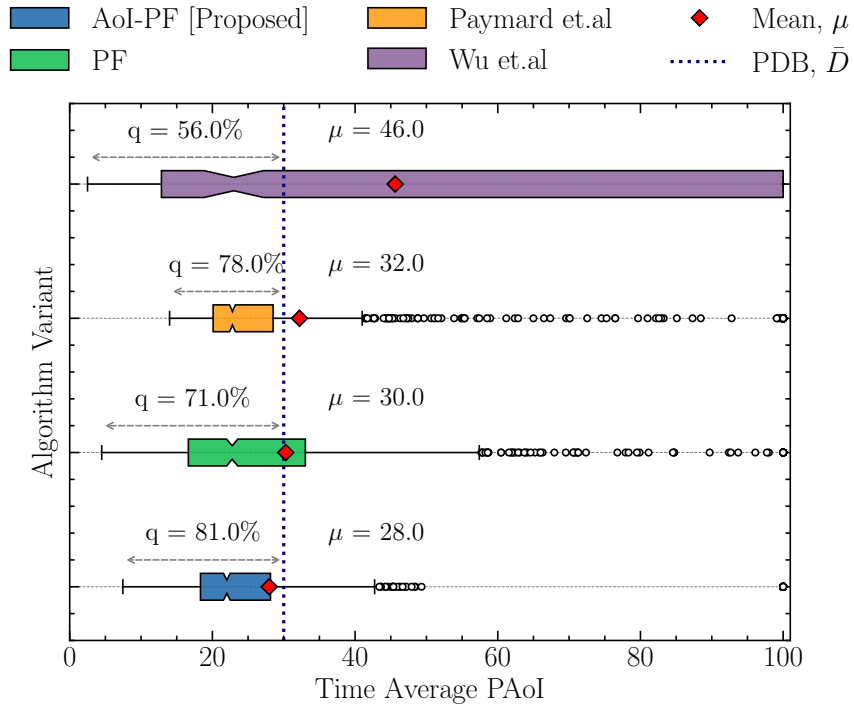


Fig. 3: PAoI distribution comparison

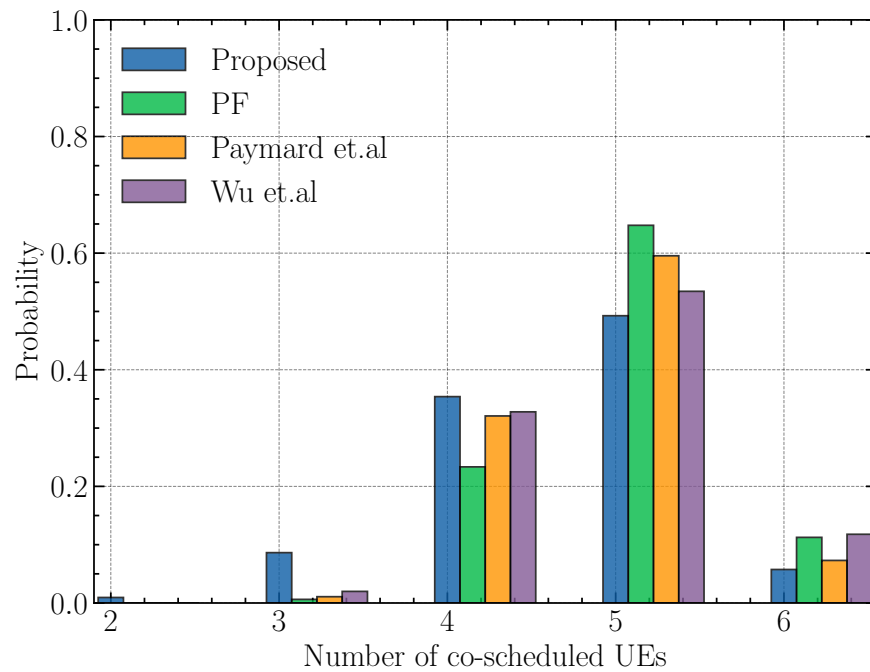


Fig. 4: Empirical distribution of co-scheduled UEs

be observed that the proposed scheduling heuristic outperforms the DRL baseline in [11] with respect to both goodput and XR capacity. This is because the DRL baseline suffers from lack of explicit interference information due to MU-MIMO and fails to adapt to XR KPIs in (6).

In Fig. 4, we compare the probability mass function (pmf) of the number of co-scheduled UEs with respect to each scheduling scheme. It can be observed that the PAoI weight from (8) regulates the number of UEs scheduled when necessary. This is in contrast to the baselines, where the number of co-scheduled UEs are concentrated more on the higher values.

VI. CONCLUSION

In this work, we proposed an iterative UE scheduling heuristic algorithm to solve the timely throughput maximization for UL MU-MIMO endowed with XR KPIs. Numerical simulations demonstrate that the proposed heuristic algorithm achieves the highest XR capacity while not sacrificing the achieved throughput. We posit the possibility of utilizing DRL techniques to reduce the computational complexity of the proposed approach.

REFERENCES

- [1] Margarita Gapeyenko, Vitaly Petrov, Stefano Paris, Andrea Marcano, and Klaus I Pedersen. Standardization of extended reality (XR) over 5G and 5G-Advanced 3GPP new radio. *IEEE network*, 37(4):22–28, 2023.
- [2] 3GPP. Study on extended reality and media service (XRM) phase 2, Release 19 SA2. Technical report, 3rd Generation Partnership Project (3GPP), Janurary 2024.
- [3] Abolfazl Amiri, Pouria Paymard, Pilar Andres-Maldonado, Stefano Paris, Klaus I. Pedersen, and Troels Kolding. Application awareness for Extended Reality services: 5G-Advanced and beyond. *IEEE Communications Magazine*, 62(8):38–44, 2024.
- [4] Jeffrey G. Andrews, Todd E. Humphreys, and Tingfang Ji. 6G takes shape. *IEEE BITS the Information Theory Magazine*, 4(1):2–24, 2024.
- [5] Hao Yin, Lyutianyang Zhang, and Sumit Roy. Multiplexing URLLC traffic within eMBB services in 5G NR: Fair scheduling. *IEEE Transactions on Communications*, 69(2):1080–1093, 2021.
- [6] Roy D. Yates, Yin Sun, D. Richard Brown, Sanjit K. Kaul, Eytan Modiano, and Sennur Ulukus. Age of information: An introduction and survey. *IEEE Journal on Selected Areas in Communications*, 39(5):1183–1210, 2021.
- [7] Kumar Saurav and Rahul Vaze. Online energy minimization under a peak age of information constraint. In *2021 19th International Symposium on Modeling and Optimization in Mobile, Ad hoc, and Wireless Networks (WiOpt)*, pages 1–8, 2021.
- [8] Pouria Paymard, Stefano Paris, Abolfazl Amiri, Troels E. Kolding, Fernando Sanchez Moya, and Klaus I. Pedersen. PDU-set scheduling algorithm for XR traffic in multi-service 5G-Advanced networks. In *ICC 2024 - IEEE International Conference on Communications*, pages 758–763, 2024.
- [9] Erkai Chen, Shengyue Dou, Shaobo Wang, Youlong Cao, and Shuri Liao. Frame-level integrated transmission for Extended Reality over 5G and beyond. In *2021 IEEE Global Communications Conference (GLOBECOM)*, pages 1–6, 2021.

- [10] Biljana Bojović, Sandra Lagén, Katerina Koutlia, Xiaodi Zhang, Ping Wang, and Liwen Yu. Enhancing 5G QoS management for XR traffic through XR loopback mechanism. *IEEE Journal on Selected Areas in Communications*, 41(6):1772–1786, 2023.
- [11] Chien-Cheng Wu, Petar Popovski, Zheng-Hua Tan, and Čedomir Stefanović. Design of AoI-aware 5G uplink scheduler using reinforcement learning. In *2021 IEEE 4th 5G World Forum (5GWF)*, pages 176–181, 2021.
- [12] Song Li, Min Li, Ruirui Chen, and Yanjing Sun. Age of transmission-optimal scheduling for state update of multi-antenna cellular internet of things. *China Communications*, 19(4):302–314, 2022.
- [13] K Pavan Srinath, Alix Jeannerot, and Alvaro Valcarce Rial. Joint resource-power allocation and UE rank selection in multi-user MIMO systems with linear transceivers. *arXiv preprint arXiv:2407.16483*, 2024.
- [14] M. Uchida and J. Kurose. An information-theoretic characterization of weighted alpha-proportional fairness. In *IEEE INFOCOM 2009*, pages 1053–1061, 2009.
- [15] 3GPP. NR; Medium Access Control (MAC) protocol specification. Technical Specification (TS) 38.321, 3rd Generation Partnership Project (3GPP), 04 2025. Version 18.5.0.
- [16] Hadley Wickham and Lisa Stryjewski. 40 years of boxplots. Technical report, had.co.nz, 2012.